

# QUANTUM SUPERPOSITION OF PARAMETRICALLY AMPLIFIED MULTIPHOTON PURE STATES WHITIN A DECOHERENCE-FREE SCHROEDINGER-CAT STRUCTURE

F.A. Bovino, F. De Martini and V. Mussi

Dipartimento di Fisica Università "La Sapienza" di Roma, Italia

October 8, 2018

## Abstract

The new process of *quantum-injection* into an optical parametric amplifier operating in *entangled* configuration is adopted to *amplify* into a large dimensionality spin- $\frac{1}{2}$  Hilbert space the quantum entanglement and superposition properties of the photon-couples generated by parametric down-conversion. The structure of the Wigner function and of the field's correlation functions shows a *decoherence-free*, multi-photon *Schroedinger-cat* behaviour of the emitted field which is largely detectable against the squeezed-vacuum noise. Furthermore, owing to its entanglement character, the system is found to exhibit multi-particle quantum nonseparability and Bell-type nonlocality properties. These relevant quantum features are analyzed for several *travelling-wave* optical configurations implying different input quantum-injection schemes. (PACS numbers: 03.65.Bz, 03.67.-a, 42.50.-p, 89.70.+c).

## 1 Introduction

The generation of classically distinguishable quantum states, a major endeavor of modern physics, has long been the object of extensive theoretical

studies. In recent times important experimental investigation with atoms has been carried out in this field by various research groups [1][2][3][4][5]. In this context it has been proved that the realization of the Schroedinger-cat program is generally challenged by an extremely rapid decoherence process due to the stochastic interactions of any freely evolving mesoscopic system with the environment [6][7]. Within the framework of quantum computation the same process has also been recognized to represent a major limitation toward the coherent superposition of the qubits carrying the quantum information [8]. In the domain of quantum optics several strategies have been proposed to overcome the problem, e.g. the back-action evasion [9] and cavity control by optical feedback [10][11]. In the present letter we present a new approach to the problem based on the amplifying / squeezing operation of the travelling wave optical parametric amplifier (OPA) operating in a novel entangled configuration and initiated by a dynamical interaction process here introduced for the first time in the framework of the nonlinear (NL) parametric amplification: *quantum-injection*. In general we may define the quantum injection process in connection with any amplifying or scattering system as the one provided by an input field whose *P – Representation* does not exist as a tempered solution [12]. In our present case the character of *quantum-injection* is provided by the subpoissonian character of a single photon in the Fock state  $n=1$  in a quantum superposition of polarization, or momentum, states. Sometimes we refer to this single particle state as the input *qubit*. This photon may belong to a couple generated by spontaneous parametric down-conversion (SPDC) e.g. in a  $\Phi$ –*phase tunable* entangled state of linear polarization  $\pi$ , defined in a Hilbert space of dimensionality  $2 \times 2$ . The SPDC process has been adopted within recent tests of violation of Bell’inequalities [13], of quantum state-teleportation [14] and of all processes generally belonging to the chapter of *nonlocal entangled interferometry* [15][16]. The key idea of the present work relates to the possibility of “amplifying” this quite interesting phenomenology to a higher dimensionality spin- $\frac{1}{2}$  Hilbert space, i.e. involving a large number of photon couples, by taking advantage of the *unitary* character of the transformation accounting for the amplification process. We show that this can be realized by a novel optical device, the quantum-injected, *entangled OPA* leading to a new *entangled* Schroedinger-cat (S-cat) configuration which may be *decoherence-free*, in the ideal case. A first account of the present work is found in Refs.[17]. This quite interesting condition, implying the linear superposition of two multi-particle, i.e. macro-

scopic *pure-states* will be investigated for two different optical travelling-wave configurations: (1) the quantum-injected non-degenerate OPA and (2) the quantum-injected mode-degenerate OPA. Both schemes will be analyzed theoretically by two different and complementary approaches. Accordingly, the paper is organized as follows:

First, the dynamical unitary evolution of the input qubit providing the quantum injection will be analyzed in the details for the two configurations in Sections 2 and 3, respectively. Second, the general approach will be followed by an *exact*, closed form evaluation of the Wigner function, in Sections 4 again for both configurations. The details of all calculations will be given for the more complex and elaborate configuration (1), for generality. Rather surprisingly, we shall see that the formal expression of the Wigner function is found the same for both configurations in spite of the somewhat different dynamics and of the different signification of the variables appearing in the resulting expression. This may emphasize the formal role taken by the common single-photon quantum injection scheme within the quantum analysis. In any case this allows an interesting unifying Wigner function analysis showing, for both configurations, the relevant multi particle quantum superposition properties of the S-cat. Third, a theory of the *first-order* optical correlation functions of the parametrically generated field, given in Section 5 suggests, for both cases, a straightforward first-order interferometric method for a direct single-beam detection of the S-cat. In addition, the detailed theoretical investigation of the *second-order* inter-mode correlation function leads to a Bell-type multi-photon quantum nonlocal behaviour of the emitted field. At last, a new multi-particle Bell-inequality experiment will be considered.

## 2 Quantum Injection in the non-degenerate Optical Parametric Amplifier. Amplification of quantum entanglement.

Consider the diagram shown in Figure 1, a diagram suggested by an actual experimental investigation presently being carried out in our Laboratory. Two equal and equally oriented NL crystals, e.g., beta-barium-borate (BBO) cut for Type II phase matching are excited by two beams derived from a common UV laser beam at a wavelength (wl)  $\lambda_p = 2\pi |\mathbf{k}_p|^{-1}$ . Crystal 1 is

the SPDC source of  $\pi$ -*entangled* photon couples emitted, with wl  $\lambda = 2\lambda_p$  over the modes  $\mathbf{k}_1, \mathbf{k}_3$  determined by two fixed pinholes.

Figure 1: Optical configuration of the quantum-injected, entangled optical parametric amplifier realizing the process of multiphoton quantum superposition. The SPDC quantum injector is provided by a type II  $\Phi$ -phase tuneble generator of linear polarization ( $\pi$ )-entangled photon couples. The crystal realizing the OPA action is cut for type II, noncollinear phase matching and is equal to the one realizing SPDC. The detection system consists of the of a birefringent plate  $\Psi$ , a  $\pi$  rotator  $R(\varphi)$ , a polarizing beam-splitter PBS and two cooled photomultipliers.

The SPDC quantum-injector is provided by a Type II  $\Phi$  – *phase tunable* generator of linear polarization ( $\pi$ )-entangled photon couples. The crystal realizing the OPA action is cut for Type II, noncollinear phase matching and is equal to the one realizing SPDC. The detection system consists of a birefringent plate  $\Psi$ , a  $\pi$  – *rotator*  $R(\varphi)$ , a polarizing-beam-splitter PBS and two cooled photomultipliers. In the experiment a similar system is inserted on mode  $\mathbf{k}_2$ . We found that the entanglement phase  $|\Phi|$  of the output state of the couple can be easily tuned over the range  $0 - \pi$  by rotating by an angle

$\psi$  the crystal around the excitation axis  $\mathbf{k}_p$ ,  $\Phi(\psi)$  being a linear function [16]. In order to prevent any EPR type state reduction that may affect the overall superposition process and then destroy the S-cat at the outset, the photon emitted over the output mode  $\mathbf{k}_3$  is filtered by a polarization analyzer with axis oriented at  $45^\circ$  to the horizontal (t.h.) before being detected by  $D_3$  [18]. An alternative solution for quantum injection, successfully tested in the experiment, is provided by a Type I NL crystal 1 feeding the OPA by a single photon with  $\pi$  oriented at  $45^\circ$ , the other photon exciting  $D_3$  without any  $\pi$ -selection. In both cases, a click at  $D_3$  opens a gate selecting all registered outcomes, thus providing the *conditional* character of the overall experiment. The photon emitted over  $\mathbf{k}_1$  provides the quantum-injection into the OPA, physically consisting of the other NL crystal. The input state to our amplifier system may be expressed in terms of superposition of Fock states associated with the modes  $\mathbf{k}_j (j = 1, 2)$  and with the two  $\pi$  components respectively parallel and orthogonal (t.h.):

$$|\Psi_0\rangle = 2^{-\frac{1}{2}} |0\rangle_{2\perp} \otimes |0\rangle_{2\parallel} \otimes \left[ |1\rangle_{1\perp} \otimes |0\rangle_{1\parallel} + e^{i\Phi} |0\rangle_{1\perp} \otimes |1\rangle_{1\parallel} \right] \quad (1)$$

For a Type II NL crystal operating in noncollinear configuration the overall amplification process taking place over  $\mathbf{k}_j$  is contributed by two equal and independent amplifiers  $OPA_A$  and  $OPA_B$  inducing unitary transformations respectively on two couples of time dependent field operators:  $(\hat{a}_1(t) \equiv \hat{a}_{1\perp}, \hat{a}_2(t) \equiv \hat{a}_{2\parallel})$  and  $(\hat{b}_1(t) \equiv \hat{a}_{1\parallel}, \hat{b}_2(t) \equiv \hat{a}_{2\perp})$  for which, at the initial time of the interaction,  $t = 0$ , is  $[\hat{a}_i(0), \hat{a}_j(0)^\dagger] = [\hat{b}_i(0), \hat{b}_j(0)^\dagger] = \delta_{ij}$  and  $[\hat{a}_i(0), \hat{b}_j(0)^\dagger] = 0$  for any  $i$  and  $j$  and  $i, j = 1, 2$ . A quantum analysis of the dynamics of the system leads to a linear dependence of the field operators on the corresponding input quantities, e.g. for  $OPA_A$ :

$$\begin{bmatrix} \hat{a}_1(t) \\ \hat{a}_2(t)^\dagger \end{bmatrix} = \begin{bmatrix} C & S \\ S & C \end{bmatrix} \begin{bmatrix} \hat{a}_1(0) \\ \hat{a}_2(0)^\dagger \end{bmatrix} \quad (2)$$

being:  $C \equiv \cosh g, S \equiv \sinh g, g \equiv \chi t$  the *amplification gain*,  $\chi$  the coupling term proportional to the product of the  $2^{nd}$ -order NL susceptibility of the crystal and of the *pump* field, assumed classical and undepleted by the parametric interaction. The interaction time,  $t$  may be determined in our case by the length  $L$  of the NL crystal. The evolution operator for

$OPA_A$  is then expressed in the form of the unitary *squeeze operator*:  $U_A(t) = \exp[g(\widehat{A}^\dagger - \widehat{A})]$  being:  $\widehat{A}^\dagger \equiv \hat{a}_1(t)^\dagger \hat{a}_2(t)^\dagger$ ,  $\widehat{A} \equiv \hat{a}_1(t) \hat{a}_2(t)$ . A corresponding  $U_B(t)$  for  $OPA_B$  is given by the replacement  $\hat{a}_i \rightarrow \widehat{b}_i$ . By use of the overall propagator  $U_A(t)U_B(t)$  and of the disentangling theorem [20], the output state is found:

$$|\Psi\rangle \equiv G \{ |\Psi_B(0)\rangle \otimes |\Psi_A(1)\rangle + e^{i\Phi} |\Psi_A(0)\rangle \otimes |\Psi_B(1)\rangle \} \quad (3)$$

where:  $G \equiv (\sqrt{2}C^2)^{-1}$ ;  $|\Psi_B(0)\rangle \equiv \sum_{n=0}^{\infty} \sqrt{P_n} |n\rangle_{1\parallel} \otimes |n\rangle_{2\perp}$ ,  $|\Psi_A(0)\rangle \equiv \sum_{n=0}^{\infty} \sqrt{P_n} |n\rangle_{1\perp} \otimes |n\rangle_{2\parallel}$ ,  $\Gamma \equiv S/C$  and  $P_n \equiv \bar{n}^n / (1 + \bar{n})^{(1+n)} = (\Gamma^{2n}/C^2)$  is a thermal distribution accounting for the squeezed-vacuum noise with average photon number  $\bar{n} = S^2$  [12]. Details on the evaluation of (3) are given in Appendix A. below The two states expressed in (3) as:  $|\Psi_A(1)\rangle \equiv \sum_{n=0}^{\infty} \Gamma^n \sqrt{n+1} |n+1\rangle_{1\perp} \otimes |n\rangle_{2\parallel}$ ,  $|\Psi_B(1)\rangle \equiv \sum_{n=0}^{\infty} \Gamma^n \sqrt{n+1} |n+1\rangle_{1\parallel} \otimes |n\rangle_{2\perp}$  represent the effect of the one-photon quantum-injection. Since this sum is extended over the complete set of n-states the appeal to the *macroscopic* quantum coherence is justified. The output state function, written in the form  $|\Psi\rangle = [|\Psi_A\rangle + e^{+i\Phi} |\Psi_B\rangle]$  with  $|\Psi_A\rangle \equiv |\Psi_B(0)\rangle \otimes |\Psi_A(1)\rangle$  and  $|\Psi_B\rangle \equiv |\Psi_A(0)\rangle \otimes |\Psi_B(1)\rangle$  expresses the condition of quantum superposition between two *pure*, multi-particle states originating, through unitary OPA transformations, from the input single-particle state  $|\Psi_0\rangle$ , keeping in this process its original phase  $\Phi$ . In facts, any unitary transformation may generally transform but not cancel the relevant quantum properties of the input state, such as superposition and entanglement, even within a (noisy) process of particle amplification as in our case. Furthermore, most important, since  $|\Psi\rangle$  is not factorizable in terms of linear polarization  $\pi$  – *states*, it keeps his original  $\pi$  – *entanglement* character thus transferring into the multi-particle regime the striking quantum nonseparability and Bell-type nonlocality properties of the microscopic (*i.e.* 2-particle) systems [18][19]. The  $\pi$  – *entanglement* properties of the output state can be investigated experimentally either by a multi-particle Bell inequality experiment, we shall consider in Section 5, or more simply and directly by the *ad hoc* optical configuration already successfully investigated in our Laboratory for the case of a  $\pi$  – *entanglement* single photon couple [15][16]. For convenience, a layout of a possible experiment of this sort applied to our S-cat condition is reported in the inset of Figure 1.

### 3 Quantum-injected mode-degenerate OPA

Consider now the diagram shown in Figure 2: the two NL crystals, e.g., BBO cut for Type II phase-matching, are again excited by two beams derived from the common UV source at wavelength  $\lambda_p$ . Crystal 1 is again the SPDC source of couples of  $\pi$ -entangled photons with  $\lambda = 2\lambda_p$ , emitted over the two output modes  $\mathbf{k}_i$  ( $i = 1, 2$ ) determined by two fixed pinholes according to the phenomenology already discussed in the previous Section.

Here again the photon emitted over  $\mathbf{k}_1$  provides the quantum-injection into the OPA consisting of the NL crystal 2 which is now cut for *collinear* operation over the two linear polarization modes  $\mathbf{k}_{1\perp}$  and  $\mathbf{k}_{1\parallel}$ , respectively parallel and orthogonal t.h.. The photon associated with the output mode  $\mathbf{k}_2$  is filtered by a polarization analyzer with axis at  $45^\circ$  respect to the t.h. and then detected by  $D_2$ . Once again, the  $\pi$  – *analyzer* prevents any nonlocal, EPR type state reduction on the correlated mode  $\mathbf{k}_1$  and  $D_2$  generates the gate pulse providing the *conditional* character of the experiment. We may note that the input, quantum injection single-photon state:

$$|\Psi_0\rangle = 2^{-\frac{1}{2}} \left[ |1\rangle_{1\perp} \otimes |0\rangle_{1\parallel} + (\exp i\Phi) |0\rangle_{1\perp} \otimes |1\rangle_{1\parallel} \right] \quad (4)$$

is again entangled over the two polarization modes belonging to the common momentum state  $\mathbf{k}_1$ . Note, by comparison with the input state expressed by Equation 1, corresponding to the optical configuration 1, that here two channels feeding vacuum into the NL crystal 2 are missing, since in the present *collinear* configuration the  $OPA_A$  and  $OPA_B$  collapse into a single  $OPA$  and the dynamics is simplified. As we shall see in Section 5 this results in a larger signal-to-noise ratio of the output field. In order to investigate the properties of the output beam after filtering against UV, a birefringent plate  $D(\Psi)$  and a Fresnel-rhomb  $R(\varphi)$  induce respectively a field's phase delay  $\Psi = (\psi_\perp - \psi_\parallel)$  and a  $(45^\circ + \varphi)$   $\pi$ –*rotation* (t.h.). Then the two orthogonal  $\pi$  components are detected by  $D_\varphi$  and  $D_{\overline{\varphi}}$  after separation by a polarizing beam splitter PBS. This realizes a  $\pi$ –interferometer as we shall see.

We may analyze the present amplification process following the lines of the theory given in Section 2. The single  $OPA$  process induces a unitary transformation on the couple of time dependent field operators:  $\hat{a}(t) \equiv \hat{a}_{1\perp}$ , and  $\hat{b}(t) \equiv \hat{a}_{1\parallel}$  for which, at the initial time of the NL interaction,  $t = 0$ , is

Figure 2: Optical configuration of the mode-degenerate entangled quantum injected OPA realizing the process of multiphoton quantum superposition within a NL crystal cut for collinear type II phase matching. For simplicity we keep the same denomination  $k_1$  for the injection mode involving both SPDC and OPA processes.

$[\hat{a}(0), \hat{a}(0)^\dagger] = [\hat{b}(0), \hat{b}(0)^\dagger] = 1$  and  $[\hat{a}(0), \hat{b}(0)^\dagger] = 0$ . Note that the present notation for the denomination of the field operators, is *not consistent* with the one adopted in Section 1. It cannot lead to confusion but rather it is found convenient in view of the comparative discussion, in the next Section, of the final expressions of Wigner functions found for the two configurations. Here again quantum analysis of the dynamics leads to a linear dependence of the field operators on the corresponding input quantities:

$$\begin{bmatrix} \hat{a}(t) \\ \hat{b}(t)^\dagger \end{bmatrix} = \begin{bmatrix} C & S \\ S & C \end{bmatrix} \begin{bmatrix} \hat{a}(0) \\ \hat{b}(0)^\dagger \end{bmatrix} \quad (5)$$

The evolution operator is then expressed in the form of the *squeeze operator*:  $U_A(t) = \exp[g(\widehat{A}^\dagger - \widehat{A})]$  being:  $\widehat{A}^\dagger \equiv \hat{a}(t)^\dagger \hat{b}(t)^\dagger$ ,  $\widehat{A} \equiv \hat{a}(t) \hat{b}(t)$ . The use of the *disentangling theorem*[20], leads to the output state:

$$|\Psi\rangle_{OUT} = G [|\bar{n} + 1_{\perp} \otimes \bar{n}_{||}\rangle + \exp(i\Phi) |\bar{n} + 1_{||} \otimes \bar{n}_{\perp}\rangle] \quad (6)$$

where  $G \equiv (2C)^{-2}$ . There the two mutually orthogonal, interfering *pure* states are now given in the form:

$$|\bar{n} + 1_{\perp} \otimes \bar{n}_{||}\rangle \equiv \sum_{n=0}^{\infty} \Gamma^n \sqrt{n+1} |n+1\rangle_{1\perp} \otimes |n\rangle_{1||} \quad (7)$$

with  $\Gamma \equiv S/C$ . It may be useful to express the output function expressed by Equation 6 in an entangled form involving two different output  $\mathbf{k}$ -vectors. In this connection a trivial example of “entanglement swapping” may be easily realized by separating the two, single momentum  $\mathbf{k}_1$ , linear polarization modes into two, single polarization, momentum modes  $\mathbf{k}_3$  and  $\mathbf{k}_4$ , by a simple insertion of a polarizing beam splitter (PBS) right at the output of the OPA, as shown in Figure 2. In that case the state at the output of PBS is given by:

$$|\Psi\rangle_{OUT} = G [|\bar{n} + 1_{\perp 3} \otimes \bar{n}_{||4}\rangle + \exp(i\Phi) |\bar{n}_{\perp 3} \otimes \bar{n} + 1_{||4}\rangle] \quad (8)$$

$$|\bar{n} + 1_{\perp 3} \otimes \bar{n}_{||4}\rangle \equiv \sum_{n=0}^{\infty} \Gamma^n \sqrt{n+1} |n+1\rangle_{3\perp} \otimes |n\rangle_{4||} \quad (8)$$

Note that the present entangled wavefunction is quite different from the one given by Equation 3 and related to the optical configuration (1). The entanglement character of the above function can be revealed by the same experimental methods referred to at the end of Section 1.

The optical configurations presented in Figures 1 and 2 are not the only possible nor the more convenient ones. Consider for instance that the mode-degenerate, collinear optical configuration shown in Figure 2 can be easily replaced by a less elegant, *non-collinear* configuration in which the OPA, consisting of a Type II NL crystal, is fed by a quantum injection single-photon over two different input  $\mathbf{k}_j$ -vectors, say  $j = 1, 2$ , each  $\mathbf{k}_j$ -vector corresponding to either one of the two mutually orthogonal linear polarizations  $\pi_j$ . The input single-photon state is then:  $|\Psi_0\rangle = 2^{-\frac{1}{2}} [ |1\rangle_{1\perp} \otimes |0\rangle_{2||} + (\exp i\Phi) |0\rangle_{1\perp} \otimes |1\rangle_{2||} ]$ . It is easy to recognize that, in

Figure 3: Three-crystal variant of the mode non-degenerate entangled OPA configuration.

this case, we are led to the *same* results given by Equations 8 with the output mode labels 3 and 4 replaced by 1 and 2. Alternatively, the OPA may consist of a Type I crystal fed by quantum injection over the two  $\mathbf{k}_j$ -vectors with *equal* polarizations  $\pi_j$ . In this case the input state is simply expressed by  $|\Psi_0\rangle = 2^{-\frac{1}{2}} [|1\rangle_1 \otimes |0\rangle_2 + (\exp i\Phi) |0\rangle_1 \otimes |1\rangle_2]$  and again the output state is given by Equations 8.

In addition, consider the optical configuration presented in Figure 3. It is a relevant three crystal variant of the above schemes and implies a *double quantum injection* into the OPA, e.g. by adoption of two distinct SPDC processes feeding in *entangled-state* the two input modes of the common entangled amplifier,  $\mathbf{k}_j$  ( $j = 1, 2$ ) within a *double-conditional* experiment. In spite of the increased experimental complications, mainly due to the low probability of the simultaneous OPA quantum-injection processes, this new configuration may present definite advantages. For instance, the *signal to noise* ratio and then the *visibility*  $V$  of the Schroedinger-cat field are far larger than the one for the mode non-degenerate OPA, as we shall see in the

next Sections. In addition and most important, the feeding if the common entangled OPA by two *simultaneous* quantum-injection processes with different phases  $\Phi_j$  adds new interesting quantum features to the output state of the emitted field. We postpone to an *ad hoc* paper an exhaustive analysis of such interesting complex optical configuration.

## 4 Wigner Function

In order to inspect at a deeper lever the above results, consider the Wigner function of the output field for the more complex configuration 1, shown in Figure 1. Evaluate first the symmetrically-ordered characteristic function of the set of complex variables  $(\eta_j, \eta_j^*, \xi_j, \xi_j^*) \equiv \{\eta, \xi\}$ ,  $(j = 1, 2)$ :  $\chi_s \{\eta, \xi\} \equiv \langle \Psi_0 | D[\eta_1(t)] D[\eta_2(t)] D[\xi_1(t)] D[\xi_2(t)] | \Psi_0 \rangle$  expressed in terms of the *displacement* operators:  $D[\eta_j(t)] \equiv \exp[\eta_j(t)\hat{a}_j(0)^\dagger - \eta_j^*(t)\hat{a}_j(0)]$ ,  $D[\xi_j(t)] \equiv \exp[\xi_j(t)\hat{b}_j(0)^\dagger - \xi_j^*(t)\hat{b}_j(0)]$  where:  $\eta_1(t) \equiv (\eta_1 C - \eta_2^* S)$ ;  $\eta_2(t) \equiv (\eta_2 C - \eta_1^* S)$ ;  $\xi_1(t) \equiv (\xi_1 C - \xi_2^* S)$ ;  $\xi_2(t) \equiv (\xi_2 C - \xi_1^* S)$ . The Wigner function, expressed in terms of the corresponding complex phase-space variables  $(\alpha_j, \alpha_j^*, \beta_j, \beta_j^*) \equiv \{\alpha, \beta\}$  is the eight-dimensional Fourier transform of  $\chi_s \{\eta, \xi\}$ , namely:

$$W \{\alpha, \beta\} = \pi^{-8} \iiint d^2 \eta_1 d^2 \eta_2 d^2 \xi_1 d^2 \xi_2 \chi_s \{\eta, \xi\} \exp \left\{ \sum_j [\eta_j^* \alpha_j - \eta_j \alpha_j^* + \xi_j^* \beta_j - \xi_j \beta_j^*] \right\} \quad (9)$$

where  $d^2 \eta_j \equiv d\eta_j d\eta_j^*$ , etc. By a lengthy application of operator algebra and integral calculus we could evaluate analytically in closed form either  $\chi_s \{\eta, \xi\}$  and  $W \{\alpha, \beta\}$ . The corresponding detailed calculations for the optical configuration (1) are reported in the Appendix B and C. The final *exact* expression of the Wigner function is:

$$W \{\alpha, \beta\} = -\overline{W_A} \{\alpha\} \overline{W_B} \{\beta\} \left[ 1 - |e^{i\Phi} \Delta_A \{\alpha\} + \Delta_B \{\beta\}|^2 \right] \quad (10)$$

where  $\Delta_A \{\alpha\} \equiv 2^{-\frac{1}{2}}(\gamma_{A+} - i\gamma_{A-})$ ,  $\Delta_B \{\beta\} \equiv 2^{-\frac{1}{2}}(\gamma_{B+} - i\gamma_{B-})$  are expressed in terms of the squeezed variables:  $\gamma_{A+} \equiv (\alpha_1 + \alpha_2^*)e^{-g}$ ;  $\gamma_{A-} \equiv i(\alpha_1 - \alpha_2^*)e^{+g}$ ;

$\gamma_{B+} \equiv (\beta_1 + \beta_2^*)e^{-g}$ ;  $\gamma_{B-} \equiv i(\beta_1 - \beta_2^*)e^{+g}$ . The Wigner functions  $\overline{W_A}\{\alpha\} \equiv 4\pi^{-2} \exp(-[|\gamma_{A+}|^2 + |\gamma_{A-}|^2])$ ;  $\overline{W_B}\{\beta\} \equiv 4\pi^{-2} \exp(-[|\gamma_{B+}|^2 + |\gamma_{B-}|^2])$  definite positive over the 4 - dimensional spaces  $\{\alpha\}$  and  $\{\beta\}$  represent the effect of squeezed-vacuum, i.e. emitted respectively by  $OPA_A$  and  $OPA_B$  in absence of any injection. Inspection of Equation 10 shows that precisely the quantum superposition character of the injected state  $|\Psi_0\rangle$  determines the dynamical quantum superposition of the devices  $OPA_A$  and  $OPA_B$ , the ones that otherwise act as *uncoupled* and *independent* objects. From another perspective, since the quasi-probability functions  $\overline{W_A}\{\alpha\}$ ,  $\overline{W_B}\{\beta\}$  corresponding to the two macrostates  $|\Psi_A\rangle$  and  $|\Psi_B\rangle$  in absence of quantum superposition are defined in two totally separated and independent spaces, their respective "distance" in the overall phase-space of the system  $\{\alpha, \beta\}$  can be thought of as "macroscopic", as generally required by any standard S-cat dynamics in a 2 - dimensional phase-space [2]. The link between the spaces  $\{\alpha\}$  and  $\{\beta\}$  is provided by the quantum superposition term in Equation 10  $2Re[e^{i\Phi}\Delta_A\{\alpha\}\Delta_B^*\{\beta\}]$ . This term provides precisely the first-order quantum interference of the macrostates  $|\Psi_A\rangle$  and  $|\Psi_B\rangle$ . In addition, and most important, Equation 10 and Figure 3 show the non definite positivity of  $W\{\alpha, \beta\}$  over its definition space. This assures the overall quantum character of our multiparticle, quantum - injected amplification scheme [12][21].

We may recognize that these last properties of the overall Wigner function of our system do indeed coincide with the formal requirements of any Schroedinger-cat apparatus, which may be outlined as follows [7]:

(a) The ability of the system to create a first-order interference fringe pattern is a necessary but *not sufficient* condition for any authentic S-cat behaviour. The following are indeed the only two *necessary and sufficient* conditions.

(b) The Wigner function defined in the overall *phase-space* of the system *must not* be definite-positive on his definition domain [12].

(c) The two interfering macrostates, identified by two corresponding gaussian-like peaks of the Wigner function must be clearly distinguishable, i.e., the *distance* between the peaks must be larger than their average width.

Note that conditions (b) and (c) imply necessarily the system's ability to produce a first-order interference pattern while the inverse argument is not necessarily true, as said. All these formal S-cat properties are shown by the tridimensional plots of the reduced Wigner functions given in Figure 4. These are drawn for  $g = 2.5$  and for different values of the injection phase  $\Phi$ ,

in correspondence with the configuration shown in Figure 1 and investigated over the output mode  $\mathbf{k}_2$  by the detection system shown in the inset of the same Figure.

The Wigner function of the output field related to the quantum-injected *mode-degenerate OPA* considered in Figure 2 and Section 3 may be obtained by a similar theoretical analysis. In facts this one is simpler because the *collinear* optical configuration adopted within the NL interaction makes the two different amplifiers  $A$  and  $B$  of the previous case to collapse into one. It follows that the dynamics of the system, instead of being described in an eight dimensional phase-space, as in the previous case, is described here in a more handy *four dimensional* space, i.e. identified by two orthogonal  $\pi$  states of the field emitted over a *single* output mode,  $\mathbf{k}_1$ .

For the sake of completeness let's outline the theory in the *collinear* case. Assume the *phase-space variables*  $(\alpha, \alpha^*, \beta, \beta^*) \equiv \{\alpha, \beta\}$ , the conjugated variables  $(\eta, \eta^*, \xi, \xi^*) \equiv \{\eta, \xi\}$  and evaluate the the *symmetrically ordered characteristic function*:  $\chi_s \{\eta, \xi\} = \langle \Psi_0 | D[\eta(t)] D[\xi(t)] | \Psi_0 \rangle$  expressed in terms of the operators  $D[\eta(t)] \equiv \exp[\eta(t)\hat{a}(0)^\dagger - \eta^*(t)\hat{a}(0)]$ ,  $D[\xi(t)] \equiv \exp[\xi(t)\hat{b}(0)^\dagger - \xi^*(t)\hat{b}(0)]$  where  $\eta(t) \equiv (\eta C - \eta^* S)$ ;  $\xi(t) \equiv (\xi C - \xi^* S)$  and  $\hat{a}(0)$ ,  $\hat{b}(0)$  are the field operators associated to the two orthogonal input  $\pi$  modes. The Wigner function is the fourth dimensional Fourier transform of  $\chi_s \{\eta, \xi\}$ .

Once again, it is evaluated analytically in *closed form* and the result is found to reproduce exactly the one expressed by Equation 10, after a previous multiplication by  $\pi^2/4$ . This unexpected result reached by the analysis of two entirely different optical configurations suggests that the actual form of  $W \{\alpha, \beta\}$  given by Equation 10 is indeed determined by the peculiar character of the single-photon *quantum-injection* process which is common to both configurations. Of course the parameters appearing in the expression of  $W \{\alpha, \beta\}$  given by Equation 10 in correspondence with the *collinear* case are now to be re-defined appropriately:  $\gamma_{A+} \equiv (\alpha + \beta^*)e^{-g}$ ,  $\gamma_{A-} \equiv i(\alpha - \beta^*)e^{+g}$ ,  $\gamma_{B+} \equiv (\beta + \alpha^*)e^{-g}$ ,  $\gamma_{B-} \equiv i(\beta - \alpha^*)e^{+g}$ .

Figure 4: Tridimensional plots of the Wigner function of the amplified field on mode  $\mathbf{k}_2$  at the output of the quantum injected mode non-degenerate OPA as function of the *squeezed* variables:  $X = (\alpha + \beta^*)e^{-g}$ ;  $Y = i(\beta - \alpha^*)e^{+g}$ , for a parametric gain  $g=2.5$  and:  $\Phi = 0, \pi/2, \pi$ .

## 5 Field-Correlation Functions

Relevant information about the quantum mechanical features of the quantum-injected OPA systems at hand are also revealed by the  $1^{st}$  and  $2^{nd} - order$  correlation functions of the output fields for both optical configurations (1) and (2) corresponding repectively to the mode non-degenerate and to the mode-degenerate cases [12]. Let's analyze both cases in correspondence with the photo-detection measurements of the output fields carried out by apparatuses equal to the one appearing in the Inset of Figure1. Such measurement devices work as follows. Before detection over the output momentum mode  $\mathbf{k}_j$  ( $j = 1, 2$ ) the fields are phase-shifted by  $\Psi_j = (\psi_{j\perp} - \psi_{j\parallel})$  by a birefringent plates and filtered by  $\pi$ -analyzers with axes oriented at the angles:  $45^0 + \varphi_j$  (t.h.). Each  $\pi$ -analyzer may consist of the combination of a Fresnel-rhomb  $\pi$ -rotator,  $R(\varphi)$  and of a polarizing beam splitter, PBS: Figures 1 and 2. The field associated with the mode  $\mathbf{k}_j$  is detected at the space-time positions  $x_j$  by two *linear* detectors  $D_{j\varphi}$  and  $D_{j\bar{\varphi}}$  with  $\bar{\varphi} \equiv \varphi + 90^0$ .

The  $1^{st} - order$  correlation-functions  $G_j^{(1)}(x_j, x_j) \equiv \langle \Psi_0 | \widehat{N}_j(t) | \Psi_0 \rangle$  are ensemble averages of the number operators  $\widehat{N}_j(t) \equiv \widehat{c}_j^\dagger(t) \widehat{c}_j(t)$  written in terms of the the detected output fields:  $\widehat{c}_j(t) \equiv [\xi_j^- \widehat{a}_j(t) + \xi_j^+ \widehat{b}_j(t)]$ ,  $[\widehat{c}_i(t), \widehat{c}_j^\dagger(t)] = \delta_{ij}$ ,  $\xi_j^+ \equiv 2^{-\frac{1}{2}}(\cos \varphi_j + \sin \varphi_j) \exp(i\psi_{j\beta})$ ,  $\xi_j^- \equiv 2^{-\frac{1}{2}}(\cos \varphi_j - \sin \varphi_j) \exp(i\psi_{j\alpha})$ , where  $\psi_{j\alpha}, \psi_{j\beta}$  are phase-shifts induced by the birefringent plate on the fields  $\widehat{a}_j(t)$ ,  $\widehat{b}_j(t)$ . These fields are determined by the linear transformations given by Equations 2 and 5 for the two configurations. In our cases  $G_j^{(1)}$  show the expected superposition character of the output field with respect to the  $\pi$ -rotation angles  $\varphi_j$  and to the  $\Delta_j^\pm \Phi \equiv (\Phi \pm \Psi_j)$  being  $\Phi$  the phase affecting the field's output entangled state expressed by Equations 3 and 6. The explicit evaluation of the first order functions for zero time delay leads to the following results in correspondence with the optical configurations (1) and (2).

The  $2^{nd} - order$  functions  $G_{ij}^{(2)}(x_i, x_j; x_j, x_i) \equiv \langle \Psi_0 | : \widehat{N}_i(t) \widehat{N}_j(t) : | \Psi_0 \rangle$  are also found for simultaneous photo-detection processes on two equal or different  $\mathbf{k}$ -modes  $i, j$  ( $i, j = 1, 2$ ).

## 5.1 Mode non-degenerate OPA:

The  $1^{st} - order$  correlation functions are found to be expressed by:  $G_1^{(1)} = \bar{n} + \frac{1}{2}(\bar{n} + 1)[1 + \cos(2\varphi_1) \cos \Delta_1^- \Phi]$ ,  $G_2^{(1)} = \bar{n} + \frac{1}{2} \bar{n}[1 + \cos(2\varphi_2) \cos \Delta_2^+ \Phi]$ .

These averages are related correspondingly to photodetection measurements carried out over the output modes 1 or 2 by the detection apparatus shown in the Inset of Figure 1. We may compare these results with the corresponding averages over the input *vacuum state*, i.e., in absence of any quantum-injection process. These averages are found to be independent of  $\varphi_j$  and  $\Delta\Psi$ , as expected and account for the unavoidable, *squeezed vacuum* quantum noise affecting our active parametric method:  $G_{1,vac}^{(1)} = G_{2,vac}^{(1)} = \bar{n}$ . By this comparison we obtain the *signal-to-noise-ratio* related to the Schroedinger-cat detection:  $s/n = 2$ , for  $\Delta_j^- \Phi = \varphi_j = 0$ . The above result immediately suggests a  $1^{st}-order$   $\pi$ -interferometric method for S-cat detection on a *single*  $\mathbf{k}_j$  beam, with *visibility*:  $V = (G_{\max}^{(1)} - G_{\min}^{(1)})/(G_{\max}^{(1)} + G_{\min}^{(1)}) \geq \frac{1}{3}$ . The Wigner function plotted in Figure 4 refer to the output field detected by this method on the mode  $\mathbf{k}_2$ . Note that the average *difference* between the signals obtained at the output of the detectors  $D_{j\varphi}$  and  $D_{j\bar{\varphi}}$  placed at the output arms of PBS of the apparatus, Figure 1 inset, operating on the output mode  $\mathbf{k}_j$ , expresses directly the *fringe pattern* related to the  $1^{st} - order$  interference between the two S-cat macrostates. For instance for  $j = 2$ , we have:  $G_2^{(1)}(\varphi_2) - G_2^{(1)}(\bar{\varphi}_2) = \bar{n} \cos(2\varphi_2) \cos \Delta_2^+ \Phi$ . The  $2^{nd} - order$  functions  $G_{ij}^{(2)}(x_i, x_j; x_j, x_i) \equiv \langle \Psi_0 | : \widehat{N}_i(t) \widehat{N}_j(t) : | \Psi_0 \rangle$  are also found:  $G_{11}^{(2)} = 2\bar{n} \{ \bar{n} + (\bar{n} + 1)[1 + \cos(2\varphi_1) \cos \Delta_1^- \Phi] \}$ ;  $G_{22}^{(2)} = 2\bar{n}^2 \{ 1 + [1 + \cos(2\varphi_2) \cos \Delta_2^+ \Phi] \}$ ;  $G_{12}^{(2)} = 2\bar{n}^2 + \bar{n}/2 + \bar{n}[(\bar{n} + 1) \cos(2\varphi_1) \cos \Delta_1^- \Phi] + \bar{n}(\bar{n} + 1/2) [1 + \cos(2\varphi_2) \cos \Delta_2^+ \Phi] + \bar{n}(\bar{n} + 1) \{ [1 + \cos \Delta\Psi] \cos^2 \Delta\varphi^- + [1 - \cos \Delta\Psi] \sin^2 \Delta\varphi^+ \}$  where:  $\Delta\varphi^\pm \equiv (\varphi_1 \pm \varphi_2)$ ,  $\Delta\Psi \equiv (\Psi_1 + \Psi_2)$ . We may easily prove, e.g. for all  $\Delta_j^\pm \Phi = \varphi_j = 0$ , that our system realizes the *maximum* quantum mechanical violation of the Cauchy-Schwarz inequality which generally holds in semi-classical field theory:  $[g_{12}^{(2)}(0)]^2 \leq g_{11}^{(2)}(0) g_{22}^{(2)}(0)$  being:  $g_{ij}^{(2)}(0) \equiv G_{ij}^{(2)}(0) [G_i^{(1)}(0) G_j^{(1)}(0)]^{-1}$  [12]. Furthermore, the given expression of  $G_{12}^{(2)}$  shows the effects of the *multiparticle* quantum nonseparability and Bell-type nonlocality, contributed by the terms proportional to  $\cos(\Delta\varphi^\pm)$  and  $\cos \Delta\Psi$ . This is a most relevant manifestation of the nonlocality properties of our quantum injected, *entangled* parametric system [18][19].

## 5.2 Mode-degenerate OPA

The analysis above can be repeated for the simpler dynamics of the *collinear* case, configuration (2). The results are:

$1^{st}$ -order correlation function:  $G^{(1)}(\varphi) = \bar{n} + (\bar{n} + \frac{1}{2})[1 + \cos(2\varphi) \cos \Delta\Phi]$ , with  $\Delta\Phi \equiv (\Psi - \Phi)$ . This leads to an *interference fringe visibility*:  $V = (G_{max}^{(1)} - G_{min}^{(1)})/(G_{max}^{(1)} + G_{min}^{(1)}) \geq \frac{1}{2}$ , for  $\Delta\Phi \equiv 0$ . Note that in the collinear case  $V$  is larger by a factor 1.5 respect to the noncollinear case, a result due to the absence in the dynamics of the input vacuum fields contributions over the mode  $\mathbf{k}_1$ , Figure1. The absence of an input vacuum field on the idler mode is a most favorable condition shared also by the three-crystal OPA configuration shown in Figure 3. Again the *fringe pattern* related to the  $1^{st}$  order interference between the two S-cat macrostates is determined by the difference:  $G^{(1)}(\varphi) - G^{(1)}(\bar{\varphi}) = \bar{n} \cos(2\varphi) \cos \Delta_2^+ \Phi$ .

The  $2^{nd}$ -order correlation functions  $G_{\varphi,\varphi'}^{(2)} \equiv \langle \Psi_0 | :[\hat{N}(t)]_\varphi [\hat{N}(t)]_{\varphi'} : | \Psi_0 \rangle$  may also be measured by use of the detectors  $D_\varphi$  and  $D_{\bar{\varphi}}$ , Figure2.. Their expressions are given here for completeness:  $G_{\varphi,\varphi}^{(2)} = 6\bar{n}^2 + 2\bar{n} + 3\bar{n}(\bar{n} + 1) \cos^2(2\varphi) + 2\bar{n}(3\bar{n} + 2) \cos(2\varphi) \cos \Delta\Phi$ ;  $G_{\varphi,\bar{\varphi}}^{(2)} = 2\bar{n}(3\bar{n} + 2) - 3\bar{n}(\bar{n} + 1) \cos^2(2\varphi)$ .

## 6 Decoherence. Conclusions.

The virtual absence of any effective decoherence within the travelling-wave (TW) parametric process we are considering may be understood by the following argument. Our Schroedinger-cat system does not consist of a *free* excitation, a condition common to *all* S-cats considered thus far in the literature. It consists in fact of a *driven* excitation which it is strongly coupled with a *continuously re-phasing* environment provided by the coherent *nonlinear* polarization of the parametric process *driving* the multiphoton field in quantum superposition. Similar situations of coherence persistence *in spite* of dissipation are often encountered in physics of the *nonlinear* dynamical systems, e.g., in solid state nonlinear spectroscopy. A nice example is provided there by the nonlinear generation of surface-polaritons or plasmons in strongly light absorbing semiconductors or metals [22]. In spite of any arbitrarily large damping of the medium, high intensity and *strictly nondecaying*, *driven* polariton waves may be nonlinearly generated over arbitrarily

large distances and times while the related *free* waves, that originate at the boundaries from the driven ones, die out quickly according to the linear optical properties of the medium. Note that in the *linear* regime, i.e. where the only driving force is the linear polarization, the two kinds of waves coincide and are damped at the same rate. We believe that the above interpretation is generally valid for any kind of dissipative process, e.g. damping, de-phasing and de-coherence. Since this one is a most disruptive process for quantum coherence in complex systems, e.g. in the domain of *quantum computation*, our results would then suggest the *nonlinear* interaction among the information carrying particles as a most efficient solution toward a large scale implementation of the new methods [23]. Of course any single photon loss event, mainly contributed in the present TW case by stray reflections, implies an elementary decoherence process. In our laboratory experiment two equal 1mm thick, BBO crystals are excited by 0.8 picosecond pulses at  $\lambda_p = 400\text{nm}$  second-harmonic-generated by a mode-locked Ti : Sa laser at a 76 MHz repetition rate with an average power  $\approx 0.3\text{W}$ . The detection system, consisting of two linear photodetectors connected to an electronic correlator, is equal to the one shown by Figure1 inset, but for the absence of the birefringent plate. The initial phase is:  $\Phi = 0$ . All surfaces are treated by special AR coatings resonant at the working  $\lambda = 800\text{nm}$  with an overall transmittivity:  $T \approx 99.60\%$ . This figure implies the loss of a single photon every  $\gtrsim 20$  pulses with the generation of  $\bar{n} \approx 10$  per pulse. This would make our S-cat experiment quite feasible. Note in this connection that the *travelling-wave* case is quite superior to the optical parametric *oscillator* (OPO) configuration where the presence of unavoidable cavity losses enhance the negative effect of all phase-disrupting processes [17].

In summary, we have given the quantum analysis of a novel nonlinear entangled TW parametric system that shows macroscopic, decoherence free, quantum superposition features that can be easily detectable. This result is reached by a smart interplay of the fundamental paradigms of modern quantum optics, i.e., *quadrature squeezing*, *multiparticle state entanglement* and *quantum nonseparability* in parametric correlations. From a foundational perspective, our method could find application within the realization of fundamental nonlocality and noncontextuality tests of quantum mechanics requiring a number of entangled particles larger than two [24]. In addition, within the fields of *quantum information* and *computation* it may represent a new way to amplify quantum coherence and entanglement over large systems

providing at the same time an elegant way to beat decoherence. Of course we are dealing here with a *noisy* system. However the "quantum-noise-reduction effect" contributed efficiently by the parametric *quadrature squeezing* may find here a successful application [12]. For many reasons we are inclined to believe that, if successful, the present project may open new and long reaching paths in some fundamental chapters of modern physics. We thank S.Branca, M.D'Ariano, G.Di Giuseppe, D.P.Di Vincenzo, G.Ghirardi for enlightening discussions, the CEE-TMR Program (Contract N.ERBMRXCT96-066) and INFN (Contract PRA97-cat) for funding.

## Appendix A: Output wavefunction

The application of the *disentangling theorem* in the context of the present work to the general input Fock state  $(|n\rangle_{1\perp} \otimes |m\rangle_{2\parallel})_{in}$  implies the use of the following transformations.

$\exp[g(\widehat{A}^\dagger - \widehat{A})](|n\rangle_{1\perp} \otimes |m\rangle_{2\parallel})_{in} = \exp\Gamma\widehat{A}^\dagger \exp(-\zeta[\widehat{A}^\dagger, \widehat{A}]) \exp(-\Gamma\widehat{A})(|n\rangle_{1\perp} \otimes |m\rangle_{2\parallel})_{in}$ , where:  $\zeta \equiv \ln C$ . Since  $[\widehat{A}^\dagger, \widehat{A}] = -\{\hat{a}_1(t)^\dagger \hat{a}_1(t) + \hat{a}_2(t)^\dagger \hat{a}_2(t) + 1\}$  the following results are found for three relevant input states.

(a)  $\exp[g(\widehat{A}^\dagger - \widehat{A})](|0\rangle_{1\perp} \otimes |0\rangle_{2\parallel}) = \exp\{-\zeta + \Gamma\widehat{A}^\dagger\}(|0\rangle_{1\perp} \otimes |0\rangle_{2\parallel}) = \sum_{n=0}^{\infty} \sqrt{P_n} |n\rangle_{1\perp} \otimes |n\rangle_{2\parallel} = |\Psi_B(0)\rangle$ , where  $P_n \equiv C^{-2}\Gamma^{2n} = \bar{n}^n/(\bar{n} + 1)^{n+1}$  expresses the *thermal distribution* of the squeezed-vacuum on the two output modes with average photon number:  $\bar{n} = S^2$ .

(b)  $\exp[g(\widehat{A}^\dagger - \widehat{A})](|1\rangle_{1\perp} \otimes |0\rangle_{2\parallel}) = \exp\Gamma\widehat{A}^\dagger \exp(-\zeta[\widehat{A}^\dagger, \widehat{A}])(|1\rangle_{1\perp} \otimes |0\rangle_{2\parallel}) = C^{-2} \sum_{n=0}^{\infty} \frac{\Gamma^n}{n!} (\hat{a}_1^\dagger)^{n+1} (\hat{a}_2^\dagger)^n (|0\rangle_{1\perp} \otimes |0\rangle_{2\parallel}) = C^{-2} \sum_{n=0}^{\infty} \Gamma^n \sqrt{n+1} (|n+1\rangle_{1\perp} \otimes |n\rangle_{2\parallel}) = |\Psi_A(1)\rangle$ .

(c)  $\exp[g(\widehat{A}^\dagger - \widehat{A})](|1\rangle_{1\perp} \otimes |1\rangle_{2\parallel}) = \exp(-3\zeta) \sum_{n=0}^{\infty} \frac{\Gamma^n}{n!} (\hat{a}_1^\dagger \hat{a}_2^\dagger)^n (|1\rangle_{1\perp} \otimes |1\rangle_{2\parallel}) - \exp(-\zeta) \Gamma \sum_{n=0}^{\infty} \Gamma^n (|n\rangle_{1\perp} \otimes |n\rangle_{2\parallel}) = C^{-3} \sum_{n=0}^{\infty} \Gamma^n (n+1) (|n\rangle_{1\perp} \otimes |n\rangle_{2\parallel}) - \Gamma |\Psi_B(0)\rangle$ . The other states appearing in Equation 3 are obtained by the same transformations upon the substitutions:  $A \leftrightharpoons B$ ,  $\parallel \leftrightharpoons \perp$  etc.

## Appendix B: Characteristic function

The symmetrically ordered characteristic function or the optical configuration (1) is evaluated by the average:

$\chi_s \{\eta, \xi\} \equiv \langle \Psi_0 | D[\eta_1(t)] D[\eta_2(t)] D[\xi_1(t)] D[\xi_2(t)] | \Psi_0 \rangle$  expressed in terms of the displacement operators:  $D[\eta_j(t)] \equiv \exp[\eta_j(t)\hat{a}_j(0)^\dagger - \eta_j^*(t)\hat{a}_j(0)]$ ;  $D[\xi_j(t)] \equiv \exp[\xi_j(t)\hat{b}_j(0)^\dagger - \xi_j^*(t)\hat{b}_j(0)]$  and of the time dependent parameters:  $\eta_1(t) \equiv (\eta_1 C - \eta_2^* S)$ ;  $\eta_2(t) \equiv (\eta_2 C - \eta_1^* S)$ ;  $\xi_1(t) \equiv (\xi_1 C - \xi_2^* S)$ ;  $\xi_2(t) \equiv (\xi_2 C - \xi_1^* S)$  where  $(\eta_j, \eta_j^*, \xi_j, \xi_j^*) \equiv \{\eta, \xi\}$ , ( $j=1, 2$ ) represents the set of the eight phase-space conjugate complex variables relative to our dynamical problem. Note that the expression of  $\chi_s \{\eta, \xi\}$  may be given in an equivalent, alternative form by use of the following results:  $D[\eta_1(t)] D[\eta_2(t)] = D[\eta_1] D[\eta_2]$  and  $D[\xi_1(t)] D[\xi_2(t)] = D[\xi_1] D[\xi_2]$  where:  $D[\eta_j] \equiv \exp[\eta_j \hat{a}_j(t)^\dagger - \eta_j^* \hat{a}_j(t)]$ ;  $D[\xi_j] \equiv \exp[\xi_j \hat{b}_j(t)^\dagger - \xi_j^* \hat{b}_j(t)]$ . These last results are obtained by use of Eqs.2

and of the well known theorem:  $\exp \widehat{A} \exp \widehat{B} = \exp(\widehat{A} + \widehat{B}) \exp \frac{1}{2} [\widehat{A}, \widehat{B}]$ . We may then evaluate the explicit expression of  $\chi_s \{\eta, \xi\}$  by use of the explicit form of the input state Eq.1 and of the well known relations involving *displacement operators*:  $D^\dagger(\alpha) = D^{-1}(\alpha) = D(-\alpha)$ ,  $D^\dagger(\alpha)\widehat{a}D(\alpha) = \widehat{a} + \alpha$ ,  $D^\dagger(\alpha)\widehat{a}^\dagger D(\alpha) = \widehat{a}^\dagger + \alpha^*$ ,  $\langle 0 | D(\alpha) | 0 \rangle = \langle 0 | \alpha \rangle = \exp(-\frac{1}{2} |\alpha|^2)$  [12]. By ensemble averaging over the two superposition terms appearing in Eq.1, the symmetrically ordered characteristic function is finally found:

$$\chi_s \{\eta, \xi\} = \left\{ 1 - \frac{1}{2} |e^{i\Phi} \eta_1(t) + \xi_1(t)|^2 \right\} \exp\left[-\frac{1}{2} \sum_j (|\eta_j(t)|^2 + |\xi_j(t)|^2)\right] \quad (11)$$

## Appendix C: Wigner Function

In view of the explicit form of  $\chi_s \{\eta, \xi\}$  the  $8^{th}$ -dimensional integral, Equation 9 is evaluated by introducing first the change of variables:  $\eta_j \rightarrow \eta_j(t)$ ,  $\xi_j \rightarrow \xi_j(t)$  and then by writing:  $\eta_j(t) \equiv x_j e^{i\varphi_j}$ ,  $\xi_j(t) \equiv y_j e^{i\varphi_j}$ ,  $d^2\eta_j \equiv d\eta_j(t)d\eta_j^*(t) = x_j dx_j d\varphi_j$ ;  $d^2\xi_j(t) \equiv d\xi_j(t)d\xi_j^*(t) = y_j dy_j d\varphi_j$  where  $|\eta_j(t)| \equiv x_j(t) \equiv x_j$  and  $|\xi_j(t)| \equiv y_j(t) \equiv y_j$ ,  $j = 1, 2$ . For integration purposes this transformation is completed by multiplication of the integrand by the determinant of the  $8 \times 8$  Jacobian matrix,  $[D_{ij}]$  with elements:  $D_{ij} = \partial \{\eta, \xi\}_i / \partial \{\eta(t), \xi(t)\}_j$  with obvious notation for the partial derivatives. It is convenient to re-define here, by a multiplication by  $\sqrt{2}$ , the linear transformations between the two sets of variables, i.e.:  $\eta_1 = \sqrt{2}[\eta_1(t)C + \eta_2^*(t)S]$ ;  $\eta_2 = \sqrt{2}[\eta_2(t)C + \eta_1^*(t)S]$ ;  $\xi_1 = \sqrt{2}[\xi_1(t)C + \xi_2^*(t)S]$ ;  $\xi_2 = \sqrt{2}[\xi_2(t)C + \xi_1^*(t)S]$ . The value of the Jacobian determinant is then found =16. By the above substitutions, the argument of the exponential in the integrand of the integral, Eq.9 may be cast in the form:  $\sum_j [\eta_j^* \alpha_j - \eta_j \alpha_j^* + \xi_j^* \beta_j - \xi_j \beta_j^*] = \sum_j [p_j \cos \varphi_j + q_j \sin \varphi_j + \bar{p}_j \cos \bar{\varphi}_j + \bar{q}_j \sin \bar{\varphi}_j]$ , where:  $p_1 = \sqrt{2}x_1[S(\alpha_2 - \alpha_2^*) + C(\alpha_1 - \alpha_1^*)]$ ;  $q_1 = i\sqrt{2}x_1[S(\alpha_2 + \alpha_2^*) - C(\alpha_1 + \alpha_1^*)]$ . The couple  $(p_2, q_2)$  is obtained by entering the substitutions:  $\alpha_1 \leftarrow \alpha_2$  and  $x_1 \rightarrow x_2$  in the expressions for  $(p_1, q_1)$ . Likewise, the couples  $(\bar{p}_1, \bar{q}_1)$  and  $(\bar{p}_2, \bar{q}_2)$  are found by the substitutions:  $\alpha_j \rightarrow \beta_j$ ,  $x_j \rightarrow y_j$  in the expressions for  $(p_1, q_1)$  and  $(p_2, q_2)$ . Consider now the following expressions:  $w_j \equiv \sqrt{p_j^2 + q_j^2} = ix_j |\delta_j|$ ,  $\bar{w}_j \equiv \sqrt{\bar{p}_j^2 + \bar{q}_j^2} = i y_j |\bar{\delta}_j|$ ,

where:  $\delta_1 \equiv 2\sqrt{2}[C\alpha_1 - S\alpha_2^*]$ ,  $\delta_2 \equiv 2\sqrt{2}[C\alpha_2 - S\alpha_1^*]$  and  $\bar{\delta}_j$  is obtained again by the substitutions:  $\alpha_j \rightarrow \beta_j$ . Turn now to Equation 9 and integrate first respect to the phases  $\varphi_j$ ,  $\bar{\varphi}_j$ . This step is accomplished by the use of the following results:

(a)  $\int_0^{2\pi} \exp(p_j \cos \varphi_j + q_j \sin \varphi_j) d\varphi_j = 2\pi \mathbf{J}_0(iw_j)$  [GR 3.937, pag.488; [25]].

(b)  $\int_0^{2\pi} \exp(p_j \cos \varphi_j + q_j \sin \varphi_j) \sin \varphi_j d\varphi_j = -i2\pi \frac{q_j}{w_j} \mathbf{J}_1(iw_j)$ .

(c)  $\int_0^{2\pi} \exp(p_j \cos \varphi_j + q_j \sin \varphi_j) \cos \varphi_j d\varphi_j = -i2\pi \frac{p_j}{w_j} \mathbf{J}_1(iw_j)$ , being  $\mathbf{J}_\nu(z)$

a Bessel function.

We may now integrate respect to  $x_j$  and  $y_j$ . For this purpose let's first evaluate the following integral involving some relevant expressions of the regular function  $F(x_j, y_j)$ :

$$I_W[F(x_j, y_j)] = \pi^{-8} \iiint d^2\eta_1 d^2\eta_2 d^2\xi_1 d^2\xi_2 F(x_j, y_j) \exp \left\{ \sum_j [(\eta_j^* \alpha_j - \eta_j \alpha_j^*) + (\xi_j^* \beta_j - \xi_j \beta_j^*)] \right\}$$

(d) Let  $F(x_j, y_j) = \exp[-\sum_j (x_j^2 + y_j^2)]$  and consider the integral [GR 4, pag. 717]:  $\int_0^\infty x^{\nu+1} e^{-\alpha x^2} \mathbf{J}_\nu(\beta x) dx = \beta^\nu (2\alpha)^{-(\nu+1)} e^{-(\beta^2/4\alpha)}$ . Assuming  $\nu = 0$ ,  $\alpha = 1$ ,  $\beta = -|\delta|$  this result leads immediately to:  $I_W[F(x_j, y_j)] = 16\pi^{-4} \exp[-\frac{1}{4} \sum_j (|\delta_j|^2 + |\bar{\delta}_j|^2)]$ .

(e) Let  $F(x_j, y_j) = (x_j^2 + y_j^2) \exp[-\sum_j (x_j^2 + y_j^2)]$  and consider the integral [GR 6.631, pag.716]:  $\int_0^\infty x^\mu e^{-\alpha x^2} \mathbf{J}_\nu(\beta x) dx = \beta^\nu \Gamma(\nu/2 + \mu/2 + \frac{1}{2}) [2^{\nu+1} \alpha^{\frac{1}{2}(\nu+\mu+1)} \Gamma(\nu+1)]^{-1} \Phi[\frac{1}{2}(\nu+\mu+1), \nu+1; -\beta^2/(4\alpha)]$  being  $\Phi(\alpha', \gamma'; z')$  a *degenerate hypergeometric* function. Apply the Kummer theorem:  $\Phi(\alpha', \gamma'; z') = e^{z'} \Phi(\gamma' - \alpha', \gamma'; -z')$  to the standard infinite series expansion:  $\Phi(\alpha', \gamma'; z') = 1 + \frac{\alpha' z'}{\gamma' 1!} + \frac{\alpha'(\alpha'+1) z'^2}{\gamma'(\gamma'+1) 2!} + \dots$  [GR 9.210 and 9.212]. Note that with the values of the parameters:  $\nu = 0$ ,  $\mu = 3$ ,  $\alpha = 1$ ,  $\beta = -|\delta|$  only the first two terms of the expansion are nonzero, i.e.  $\Phi(2, 1; -\frac{1}{4}|\delta|^2) = [1 - \frac{1}{4}|\delta|^2] \exp(-\frac{1}{4}|\delta|^2)$ . This leads to the *exact* result:  $I_W[F(x_j, y_j)] = 16\pi^{-4} [2 - \frac{1}{4}(|\delta_j|^2 + |\bar{\delta}_j|^2)] \exp[-\frac{1}{4} \sum_j (|\delta_j|^2 + |\bar{\delta}_j|^2)]$

(f) Let  $F(x_j, y_j) = x_j y_j \exp i(\varphi_j - \bar{\varphi}_j) \exp[-\sum_j (x_j^2 + y_j^2)]$  and consider the integral GR 6.631 just given at paragraph (e). With the new set of parameters:  $\nu = 1$ ,  $\mu = 2$ ,  $\alpha = 1$ ,  $\beta = -|\delta|$ , and by use of the quoted Kummer theorem within the series expansion for  $\Phi(2, 2; -\frac{1}{4}|\delta|^2)$ , the *exact* value of the integral is found:  $-\frac{1}{4}|\delta| \exp(-\frac{1}{4}|\delta|)$ . This leads to the result:  $(w_j)^{-1} \int_0^\infty x_j^2 J_1(-x_j |\delta_j|) dx_j = i(4x_j)^{-1} \exp(-\frac{1}{4}|\delta_j|)$ . A further calculation of an identical integral involving the variables  $y_j$ ,  $\bar{w}_j$ ,  $\bar{\delta}_j$  leads to the result:  $I_W[F(x_j, y_j)] = -(16\pi^{-4})\delta_j \bar{\delta}_j^* \exp[-\frac{1}{4}\sum_j (|\delta_j|^2 + |\bar{\delta}_j|^2)]$ . At last we insert the explicit expression of  $\chi_s \{\eta, \xi\}$  found in Appendix B within the integral expressed by Equation 9 and use the above results  $d, e, f$ . This leads to the final expression of  $W \{\alpha, \beta\}$  given by Equation 10.

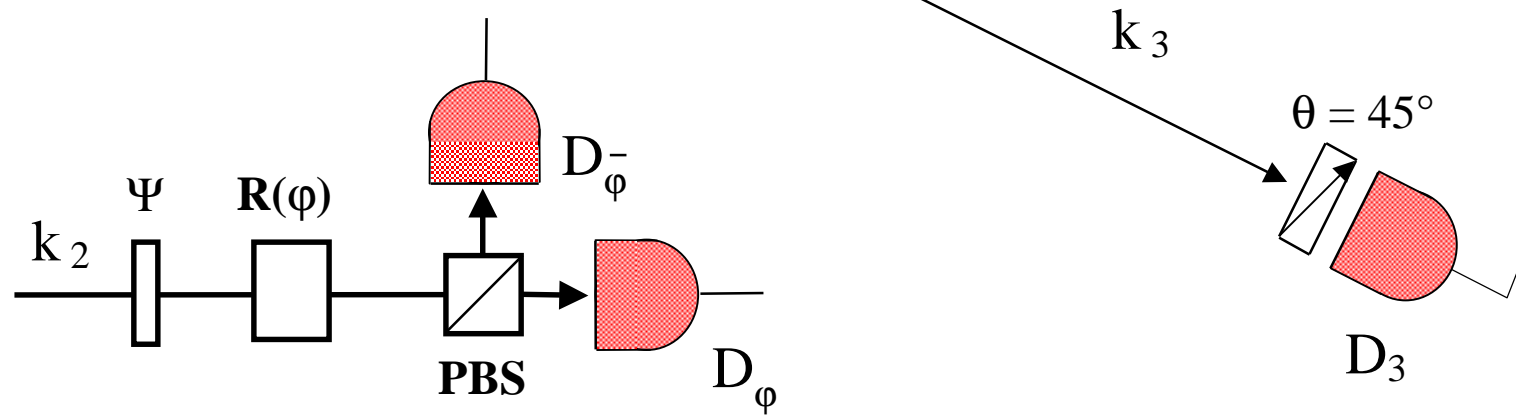
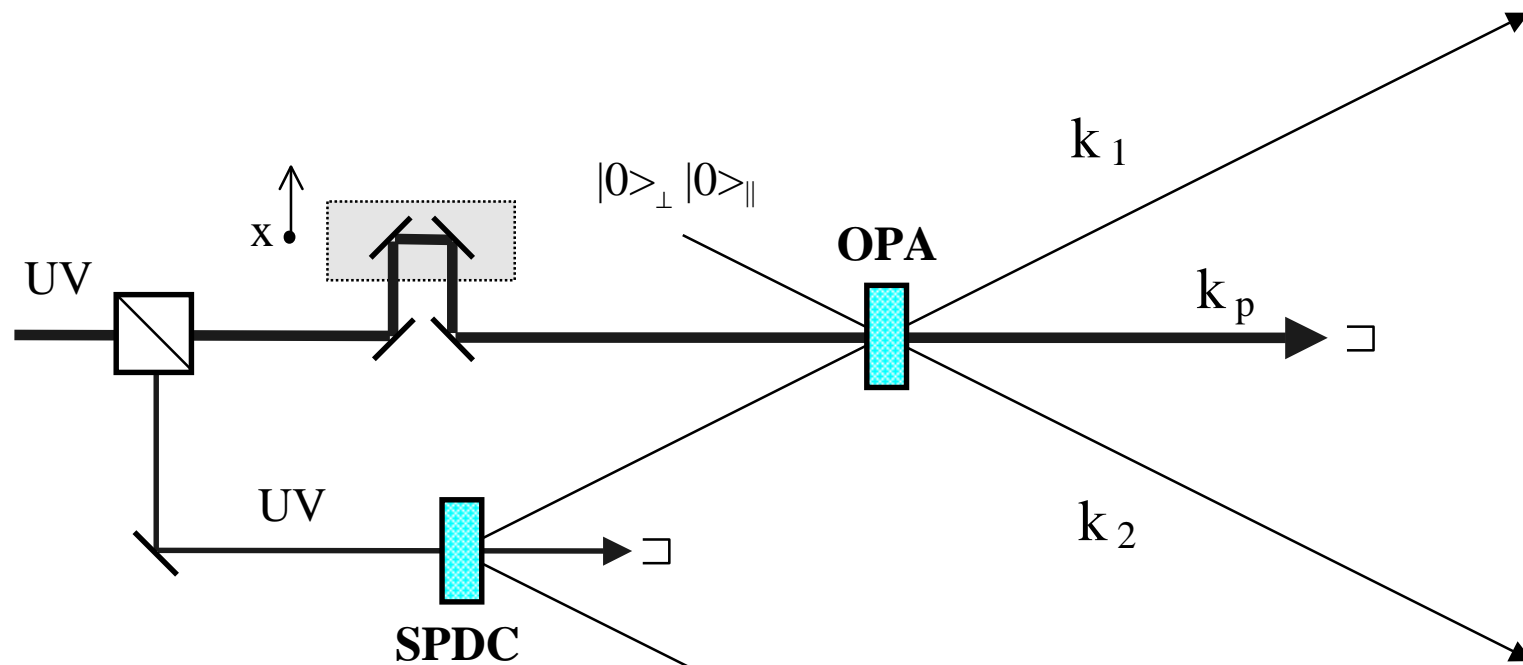
## References

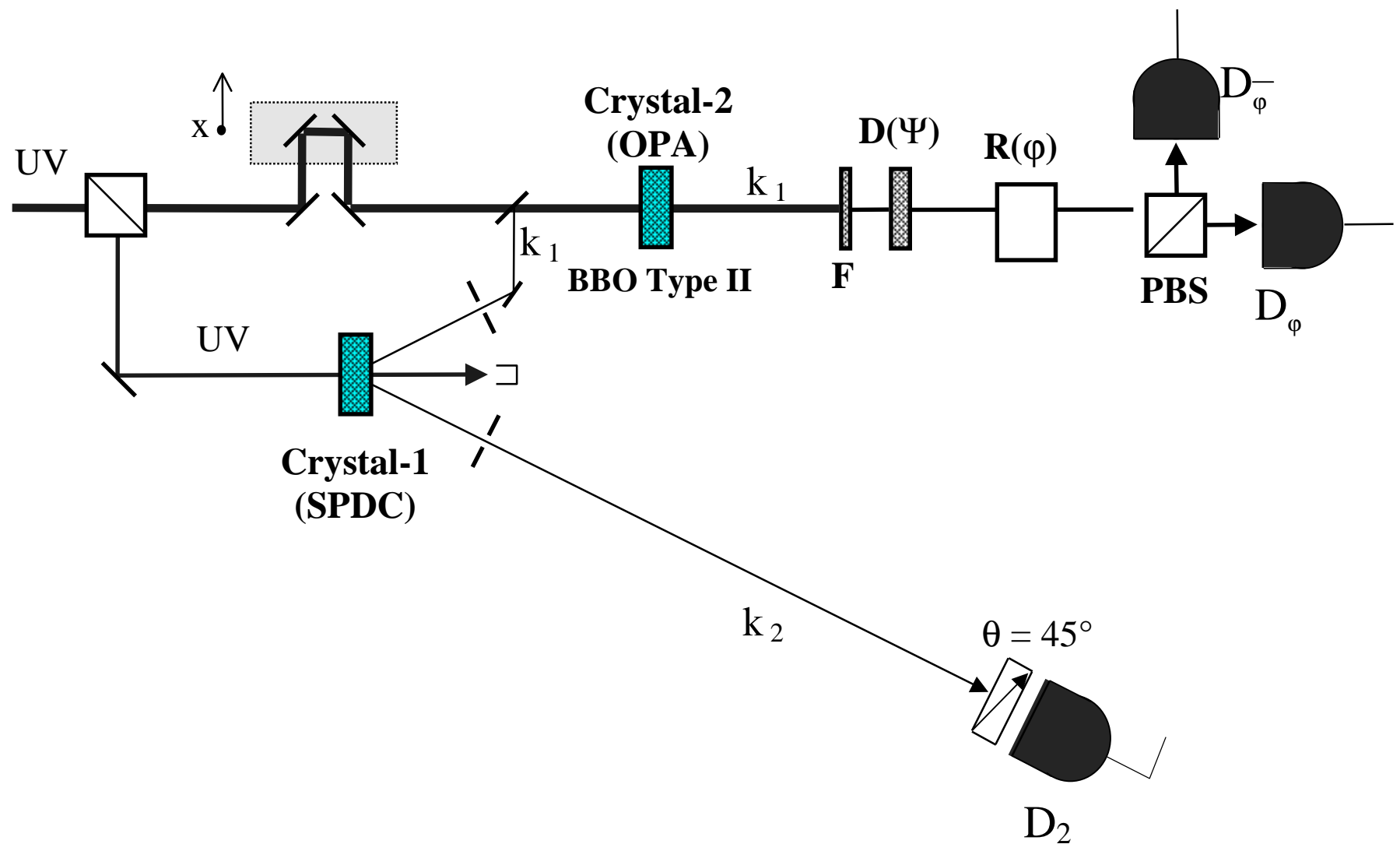
- [1] E. Schroedinger, Naturwissenschaften **23**, 807; 823; 844 (1935)
- [2] A. O. Caldeira and A. J. Leggett, Physica A **121**, 587.
- [3] C. Monroe, D. Meekhof, B. King and D. Wineland, Science 272, 1131 (1996).
- [4] M. Brune, E. Hagley, J. Dreyer, X. Maistre, A. Maali, C. Wunderlich, J. M. Raimond and S. Haroche, Phys. Rev. Lett. 77, 4887 (1996).
- [5] M. W. Noel, C. R. Stroud, Phys. Rev. Lett. 77, 1913 (1996).
- [6] D. F. Walls and G. J. Milburn, Phys. Rev. A **31**, 2403 (1985).
- [7] W. H. Zurek, Phys. Rev. D **24**, 1516 (1981); Phys. Rev. D **26**, 1862 (1982);
- [8] I. L. Chuang, R. Laflamme, P. W. Shor, W. H. Zurek, Science, 270, 1633 (1995).
- [9] S. Song, C. M. Caves and B. Yurke, Phys. Rev. A, **41**, 5261 (1990).

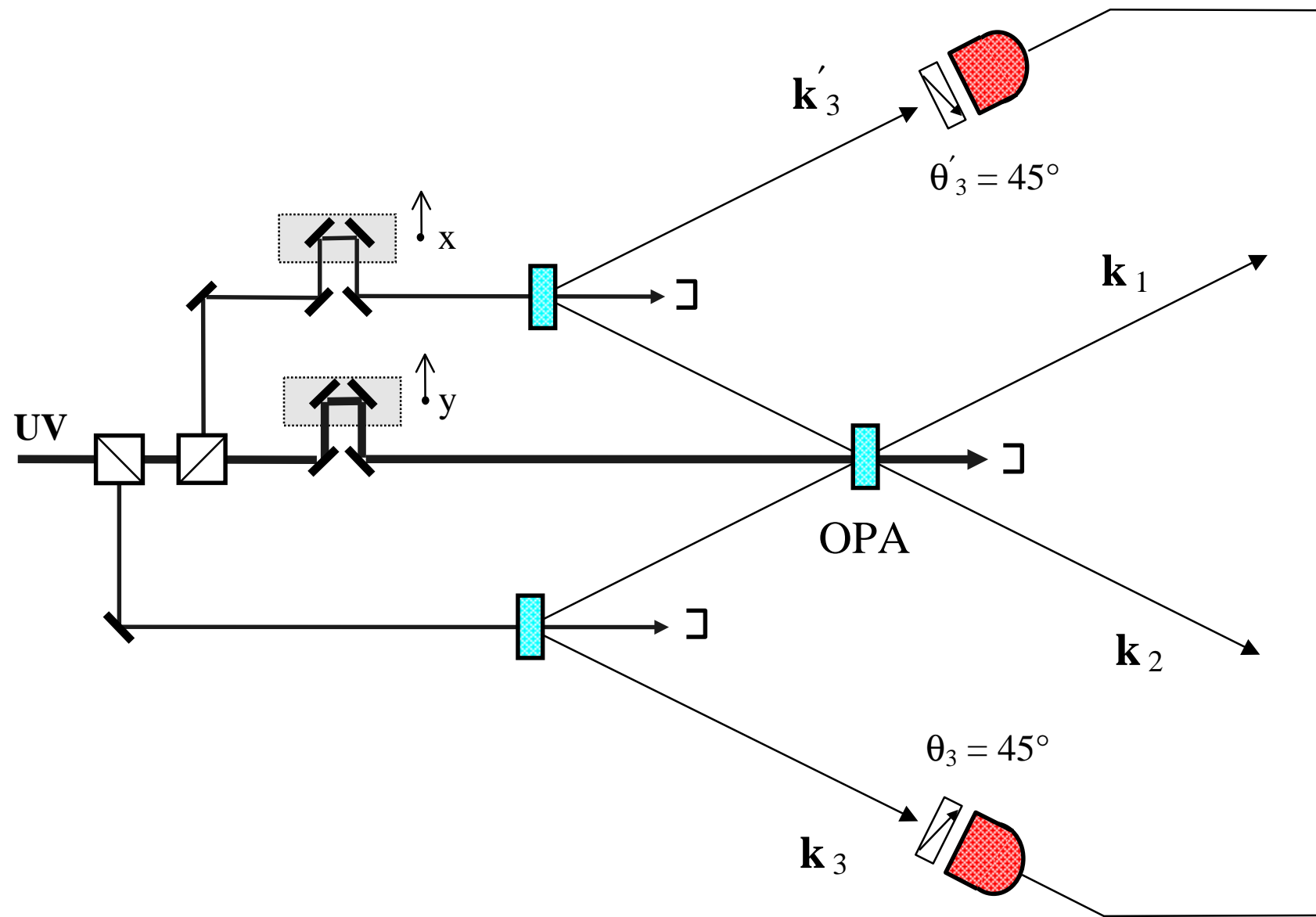
- [10] H. M. Wiseman and G. I. Milburn, Phys.Rev.A **49**, 4110 (1994).
- [11] P. Tombesi and D. Vitali, Phys.Rev.A, 50, 4253 (1994).
- [12] D. F. Walls and G. I. Milburn, *Quantum Optics* (Springer-Verlag, Berlin, 1995) Ch.5.
- [13] P. Kwiat, K. Mattle, H. Weinfurter, A. Zeilinger, A. Sergienko, Y. Shih, Phys. Rev.Lett. **75**, 4337 (1995); D. Boschi (Laurea Thesis, Università di Roma “La Sapienza”, June 1995).
- [14] D. Bouwmeester, J.W. Pan, K. Mattle, M. Eibl, H. Weinfurter and A. Zeilinger, Nature, 390, 575 (1997); D. Boschi, S. Branca, F. De Martini, L. Hardy and S. Popescu, Phys. Rev. Lett. **80**, 1121 (1998).
- [15] J. Franson, Phys.Rev.Lett. **62**, 2205 (1989); P. Kwiat, A. Steinberg and R. Chiao, Phys.Rev.A, 45, 7729 (1992); T. Larchuk, R. Campos, J. Rarity, P. Tapster, E. Jakeman, B. Saleh, and M. Teich, Phys.Rev.Lett. **70**, 1603 (1993); T.B. Pittman, D. Strekalov, A. Sergienko, M. Rubin, D. Klyshko and Y. Shih, Phys.Rev.A **52**, R3429 (1995); K. Mattle, H. Weinfurter, P. Kwiat and A. Zeilinger, Phys. Rev. Lett. **76**, 4656 (1996). D. Boschi, F. De Martini and G. Di Giuseppe in *Fundamental Problems in Quantum Theory*, ed. by Shih and Rubin Fortschritte der Physik, Vol. 46, 643, 1998.
- [16] D. Boschi, F. De Martini and G. Di Giuseppe in *Quantum Interferometry*, F. De Martini, G. Denardo and Y. Shih Eds. (VCH, Weinheim, 1996). S. Branca, D. Boschi, F. De Martini and G. Di Giuseppe, subm. to Physics Letters A. We have found experimentally that the *entanglement phase*  $\Phi$  of the SPDC generated entangled 2-photon state can be tuned by rotating the NL crystal by an angle  $\theta$  around the excitation axis  $\mathbf{k}_p$ , being  $\Phi \propto \theta$ . In BBO is found:  $\Phi/\vartheta \approx 130$  at  $\lambda = 702\text{nm}$ .
- [17] F. De Martini, Phys. Rev. Lett. **81** (1998) and: Phys.Lett. A **250**, 15(1998). A theory of the present process in a less convenient *parametric oscillator* structure is given in: F. De Martini, M. Fortunato, P. Tombesi and D. Vitali, Phys.Rev.A, May 6, 1999.
- [18] A. Einstein, B. Podolsky, N. Rosen, Phys.Rev. **47**, 777 (1935); J.S. Bell, Physics, 1, 195 (1964); Another solution for quantum injection consists

of a Type I NL crystal feeding the OPA by a photon with  $\pi$  oriented at  $45^\circ$ (t.h.), the other photon exciting  $D_3$  *without  $\pi$ -selection*. The work by X. Zou, L.Wang and L. Mandel in Phys. Rev. Lett. 67, 318, (1991) is different from the present one since there no entanglement nor amplification effects were considered.

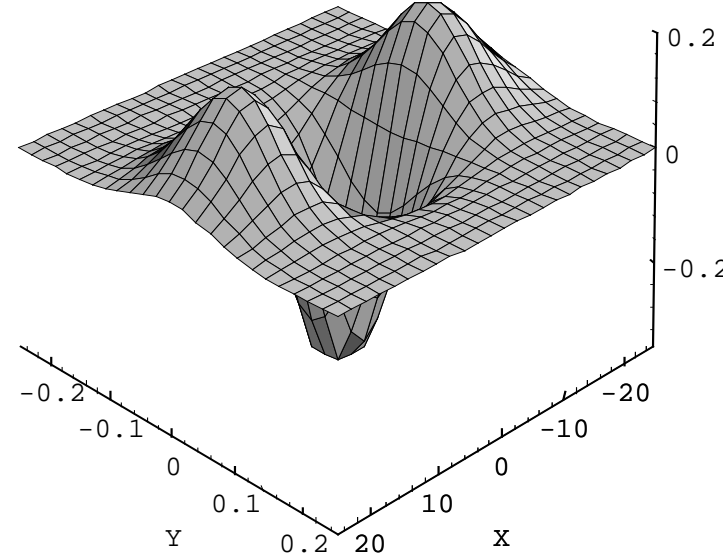
- [19] C. Su and K. Wodkiewicz, Phys. Rev. A, 44, 6097 (1991). W.L. Munro, M.D. Reid, Quantum Opt.6, 1 (1994). Owing to space limitations we postpone to another paper the analysis of a conceivable Bell-type *multiparticle* nonlocality test by our system.
- [20] M. J. Collett, Phys.Rev.A **38**, 2233 (1988).
- [21] C. W. Gardiner, *Quantum Noise* (Springer, Berlin, 1991), Ch.8.
- [22] F. De Martini and Y. R. Shen, Phys. Rev. Lett. 36, 216 (1976); F.De Martini, P. Mataloni, E.Palange,-Y.R.Shen, Phys.Rev.Lett. 37, 440 (1976); F.De Martini, M.Colocci, S.Kohn and Y.R.Shen, Phys. Rev.Lett. 38, 1223(1977).
- [23] The realization of nonlinear universal logic gates is now being considered as a sensible solution toward experimental quantum computation: D. Di Vincenzo (private comm.).
- [24] D.M. Greenberger, M.A. Horne and A. Zeilinger, Am. J. Phys. 58, 1131 (1990); N.D. Mermin, Phys.Rev.Lett. 65,1838 (1990) and: Revs. Mod. Physics, 65, 803 (1993); A. Cabello and G. Alcaine, Phys.Rev.Lett.80,1797 (1998)
- [25] I. S. Gradshteyn and I. M. Ryzhik, *Table of Integrals, Series and Products* (Academic Press, New York, 1980).



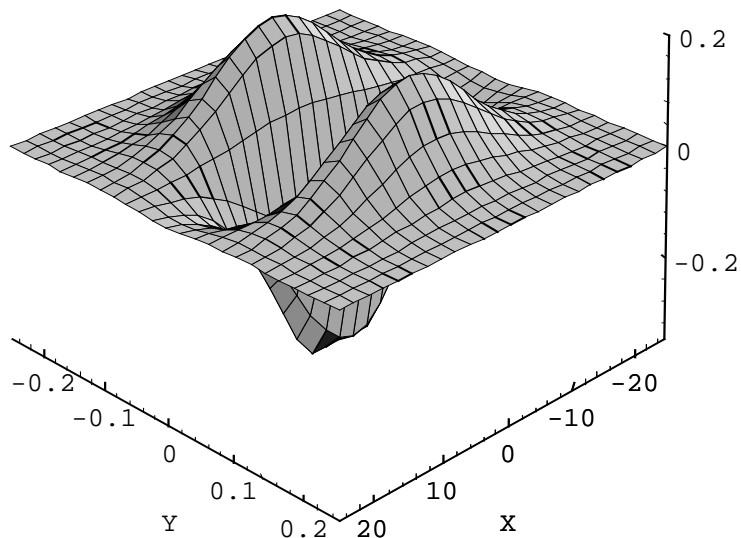




$g = 2.5$  ,  $\Phi = 0$



$g = 2.5$  ,  $\Phi = \pi$



$$g = 2.5, \Phi = \pi/2$$

